BEHAVIOUR OF OFFSHORE PILES SUBJECTED TO STORM LOADING

C.Y. Lee[1] and H.G. Poulos[2].

SYNOPSIS

This paper presents results of a limited series of model pile tests in offshore calcareous soil subjected to three different storm loadings. Attention is concentrated on the accumulation of pile displacement induced by the storm loading, and on the post-storm load capacity of the pile.

A non-linear boundary element analysis is described and is used in an attempt to predict the model test results based on soil parameters derived from earlier tests. The analysis is also employed to simulate the general cyclic behaviour of a field grouted pile test in calcareous soil. Some measure of agreement is found between predicted and measured behaviour. Finally, the analysis is used to investigate the behaviour of a hypothetical, but realistic, offshore pile subjected to a complete storm loading sequence.

INTRODUCTION

Offshore piles are usually designed not only to withstand the substantial load from the self-weight of a platform, but also the variable complex loadings caused by the environment (e.g. storm waves and earthquake). This paper investigates the behaviour of offshore piles subjected to storm-induced axial loading.

The paper presents the result of a series of tests carried out on model grouted piles in an offshore calcareous sand subjected to a scaled storm loading profile, based on data obtained for an offshore platform on the North West Shelf of Australia. The main aim is to study the accumulation of pile settlement under the irregular cyclic loading caused by the storm.

A simplified boundary element analysis with a non-linear pile-soil interface model is employed to predict the model pile test results, using soil parameters

---

[1] Research Fellow, School of Civil and Mining Engineering, University of Sydney, NSW 2006, Australia.

[2] Professor, School of Civil and Mining Engineering, University of Sydney, NSW 2006, Australia.

derived from earlier model test results (Lee & Poulos, 1990a, 1990b). Based on these soil parameters, the behaviour of a full-scale offshore pile subjected to three different complete storm loadings is investigated and compared with the model pile test behaviour.

LABORATORY SAND PREPARATION AND PILE CONSTRUCTION PROCEDURES

The model grouted pile tests were performed in a large steel consolidation vessel of internal diameter 420 mm and depth 640 mm, as shown diagrammatically in Fig. 1. The preparation procedure and the engineering properties of the offshore uncemented calcareous sand used here are described in detail by Lee & Poulos (1990b). The calcareous sand is obtained from the North Rankin offshore gas platform site on the North West Shelf of Australia. Some of the important characteristics of the soil are summarised below (Hull et al. 1988) :

A Data Acquisition System
B Loading Machine
C Proving Ring
D Displacement Transducer
E Sealing Collar
F Consolidation Vessel Lid
G Consolidation Vessel Body
H Rubber Membrane
I Rubber O-Ring
J Model Grouted Pile
K Soil
L Soft Rubber
M Brass Cap
N Top and Bottom Drainage
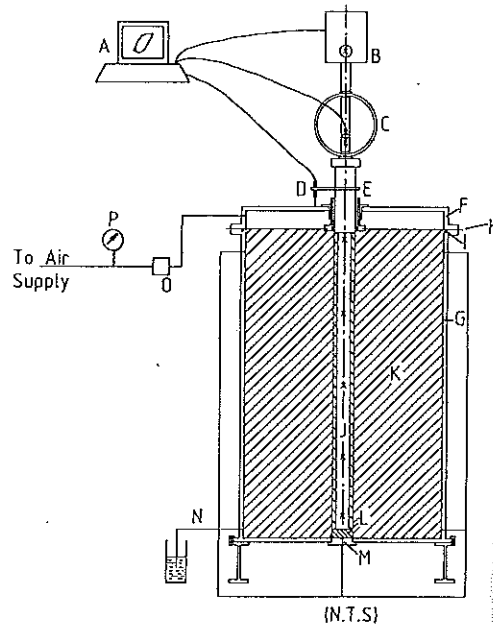O Precision Pressure Regulator
P Pressure Gauge

Fig. 1 Apparatus set-up for grouted pile tests.

Minimum density	1.19 t/m²
Maximum density	1.31 t/m³
Average carbonate content	90-97%
Origin of carbonate	bioclastic
Grain size	Medium to coarse (0.2-2 mm)
Peak effective drained Young's modulus	$(7.8 + 0.32\sigma'_c)$ MPa
Peak effective frictional angle	$(46.8 - 0.02\sigma'_c)$ degree
Drained effective Poisson's ratio	0.15

where σ'_c = effective confining pressure in kPa.

In order to obtain a fully saturated and uniform relative density throughout the soil sample, the sand was rained carefully into the consolidation vessel through water from a constant height. The construction of the grouted pile was only begun when the saturated sand had been consolidated overnight at 200 kPa overburden pressure. With the aid of a guiding device, a hole was drilled to the desired depth using a metal drill of about 47 mm diameter. The drilled hole in the soil was found to stand open without support. A 50 mm diameter 25 mm thick soft rubber plug was inserted at the bottom of the hole to minimise the base resistance developed during compression loading. The grout for the pile was prepared from Portland type B cement with a sand/cement ratio of 0.8 and a water/cement ratio of 0.7. In order to allow a 15 mm diameter aluminium rod to be smoothly inserted into the centre of the wet grout, fly-ash/cement and superplasticizer/cement ratios of 0.2 and 0.13 respectively were used with the grout. The aluminium rod provided a means of connection of the pile to the loading device and also acted as a reinforcement for the pile. When pile construction was completed, the vessel was reassembled immediately and the overburden pressure reapplied. The grouted pile was then allowed to cure for 3 to 4 days before testing. All the tests were performed under 200 kPa effective overburden pressure. The soil relative density was between 50% and 60%.

PILE TESTING PROCEDURES

Table 1 shows the three patterns of storn loading used in the model tests. The dimensionless mean and cyclic load levels for "Storm 1" are representative of the five largest "parcels" of cyclic loading of waves up to 23.2 m in height at the site of a gas platform on the North West Shelf of Australia. "Storm 2" represents the loads in "Storm 1" multiplied by a factor of 1.5, and "Storm 3" represents the loads in "Storm 1" multiplied by a factor of 2.0. For each of the three storm loadings, replicate tests were carried out. The tests are referred to as Tests 1A and

1B for Storm 1, 2A and 2B for Storm 2, and 3A and 3B for Storm 3.

All the model piles were subjected to load-controlled tension testing and only the pile shaft resistance was considered. The testing procedure was as follows :

(a) an initial static loading in tension to a specified mean load level ;

(b) cyclic loading, between predetermined limit of load levels, for a specified number of cycles. This completed a "parcel" of loading.

The process was repeated until all the parcels of loading were completed and hence the storm loading was simulated. The loading and data collection were performed by a computer-controlled data acquisition system.

Table 1 Details of Storm Loading used in Model Tests.

STORM NO.	PARCEL NO.	NO. OF CYCLES	MEAN LOAD $\frac{P}{P_u}$	CYCLIC LOAD $\frac{P}{P_u}$
1	1	20	0.244	0.070
	2	10	0.248	0.076
	3	6	0.253	0.082
	4	3	0.258	0.088
	5	1	0.267	0.100
2	1	20	0.366	0.105
	2	10	0.372	0.114
	3	6	0.380	0.123
	4	3	0.387	0.132
	5	1	0.400	0.150
3	1	20	0.488	0.140
	2	10	0.496	0.152
	3	6	0.506	0.164
	4	3	0.516	0.176
	5	1	0.533	0.200

EXPERIMENTAL RESULTS

Fig. 2 illustrates the effect of number of cycles and magnitude of the loading parcels on the accumulation of the pile displacement due to the original storm loading Storm 1. This storm loading had little effect on the pile displacement, thus indicating that the applied storm loading involved load mainly within the elastic range of the pile.

For Storm 2, where the original storm loading was factored up by 1.5, the accumulation of the pile displacement was increased, as shown in Fig. 3. It was found that the increase of pile displacement was almost linearly proportional to the number of load cycles.

However, for Storm 3, where the original storm loading was factored up by 2.0, the accumulation of pile displacement was increased significantly and the pile failed at the end of the storm, as shown in Fig. 4. When the maximum storm load was greater than 70% of the pile capacity the rate of accumulation of
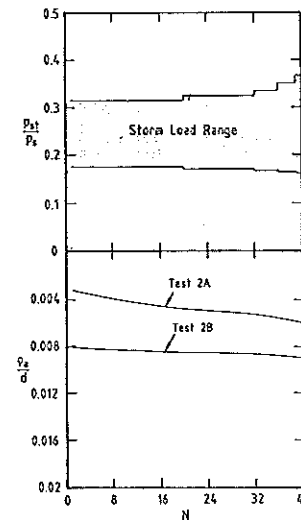

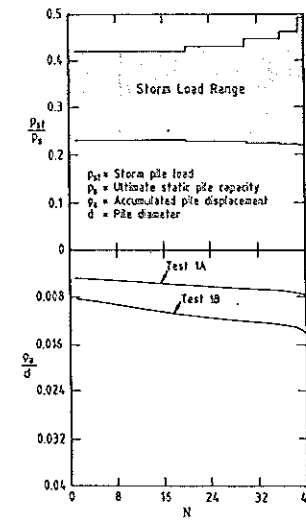Fig. 2 Model pile tests (storm No. 1).

Fig. 3 Model pile tests (storm No. 2).

pile displacement increased substantially, and the pile failed within 10 cycles.

For all three storm loadings, the replicate tests showed agreement in the general behaviour, but there was considerable difference in the magnitude of the measured axial displacement. Additional repeat tests will need to be performed to investigate this in more detail.
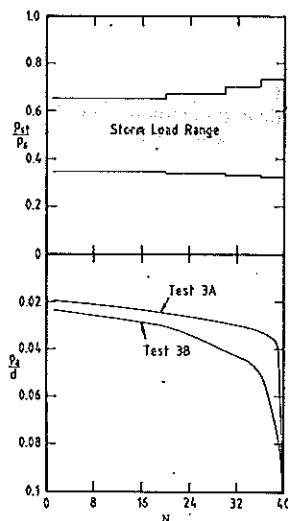

Fig. 4   Model pile tests (storm No. 3).

THEORETICAL ANALYSIS

. For the theoretical analysis, a simplified form of boundary element analysis (Poulos, 1989) was employed in which the pile is represented as an elastic cylinder and the surrounding soil mass as an elastic continuum.

The pile-soil interface behaviour is simulated by a modified Ramberg-Osgood non-linear model (Ramberg-Osgood, 1943; Hara, 1980) and the hysteresis loops developed during cyclic loading are modelled by utilising the Masing rules (Masing, 1926; Pyke, 1978), and hence the reloading and unloading can be expressed as follows :

$$E_{sc} = \frac{E_m}{\left[1 + \frac{2\alpha}{2^R} \cdot \left| \frac{p \pm p_r}{\tau_{fc}} \right|^{R-1} \right]} \qquad (1)$$

where

E_{sc} = secant soil modulus after cycling

E_m = maximum tangent soil modulus

τ_{fc} = limiting peak resistance after cycling

p = current interface stress

p_r = interface stress at the most recent point on the backbone curve at which loading is reversed

α, R = experimentally-determined parameters.

SIMULATING THE CYCLIC LOADING EFFECTS

The limiting pile skin resistance after cycling τ_{fc}, can be expressed as :

$$\tau_{fc} = D_\tau \tau_f \qquad (2)$$

where

τ_f = limiting skin resistance for static loading

D_τ = cyclic degradation factor for shaft resistance.

The degradation factor D_τ may be simulated by the modified skin friction degradation (MSFD) model (Lee & Poulos, 1990c) which at any stage employs either a cyclic displacement controlled relationship as shown in Fig. 5, or a reverse-plastic-stress controlled (Matlock & Foo, 1979) relationship, which can be expressed as :

$$D_\tau = (1 - \lambda)(D_\tau' - D_{\tau\,lim}) + D_{\tau\,lim} \qquad (3)$$

where

D_τ = current degradation factor

D_τ' = degradation factor prior to most recent application of reverse slip

$D_{\tau \lim}$ = minimum possible degradation factor

λ = degradation rate factor

Small-scale model pile tests in offshore calcareous soils (Poulos & Lee, 1988, 1989; Lee & Poulos, 1990a), show that the secant soil modulus E_{sc} after cycling decreases with number of cycles even at moderate stress levels. The secant soil modulus after cycling, may be expressed as follows :
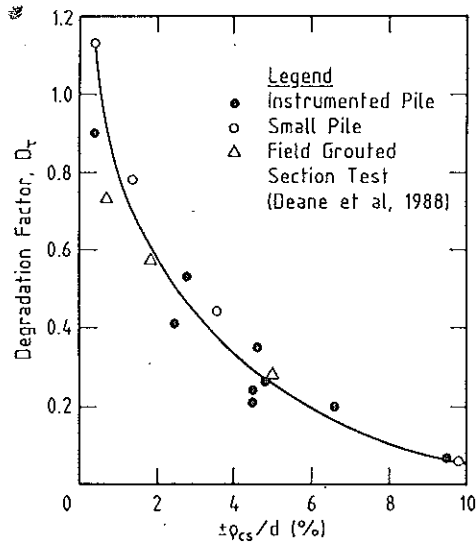

Fig. 5   Effect of normalised cyclic slip displacement on D_τ

$$E_{sc} = \{D'_{sc} - 0.5\,\theta\,x_s\,[D_{SE}]^{(1+\theta x_s)/\theta\,x_s}\}E_s \qquad (4)$$

and

$$x_s = \frac{\tau_m + 2\tau_c}{2\tau_f}$$

where

E_s = static secant soil modulus

D_{SE} = current secant soil modulus degradation factor

D'_{SE} = secant soil modulus degradation factor existing prior to the current cycle of loading

X_s = current representative stress level

τ_m = mean stress

τ_c = cyclic stress

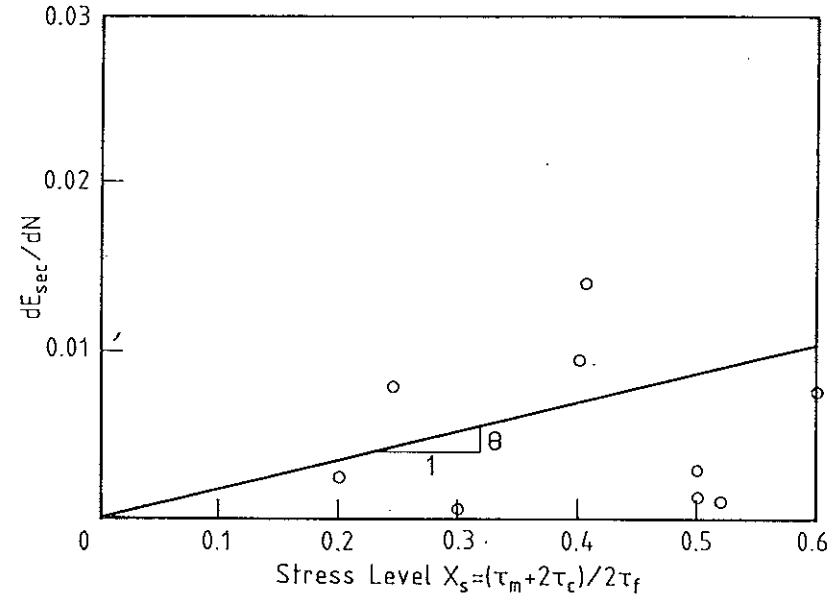θ = a degradation parameter which is a function of soil and pile types (see Fig. 6).

Fig. 6   Determination of parameter θ.

Further detail of the non-linear pile-soil model, modified skin friction degradation model (MSFD) and the secant modulus degradation model are given by Lee & Poulos (1990c).

The parameters used for the theoretical predictions were determined from earlier series of pile tests by Lee & Poulos (1990a, 1990b) and Poulos & Lee (1988, 1989), and are listed in Table 2. As can be seen from Fig. 6, the
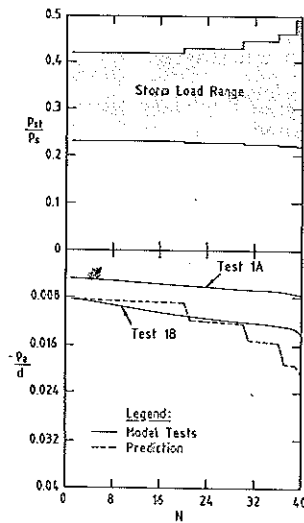
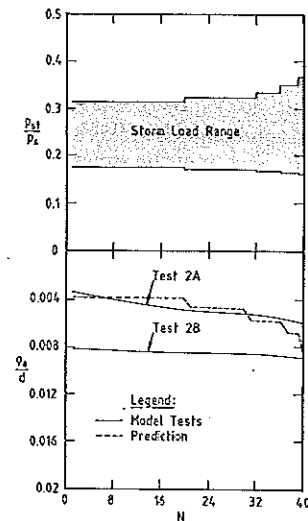Fig. 7 Measurements and
prediction for storm 1.

Fig. 8 Measurements and
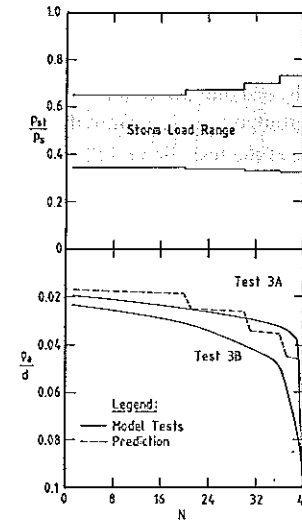prediction for storm 2.

Fig. 9 Measurements and prediction for storm 3.

assumption of a single value of the parameter is a considerable simplification, and scope exists for a wide interpretation of the value of θ.

Model Pile Tests

Fig. 7 shows that the theory overpredicts the pile settlement for the original storm loading (Storm 1). The prediction is closer to the larger of the two test results, but the predicted rate of increase in displacement at the last few cycles is higher than that measured.

For Storm 2, Fig. 8 shows that the analysis again overestimates the test results beyond the first 30 cycles.

The comparison for Storm 3 is shown in Fig. 9. The analysis slightly underestimates the test results in the first 20 cycles, but the agreement becomes closer.as the number of cycles increases.
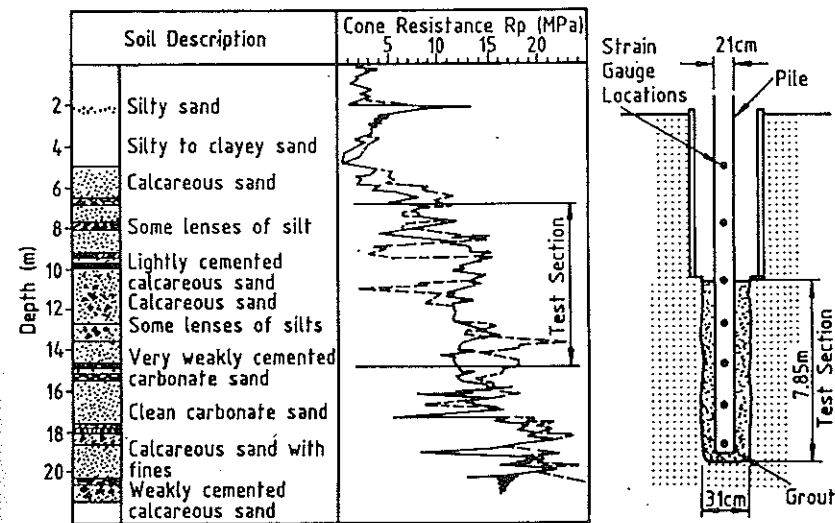

Fig. 10 IFP plouasne, brittany pile load test pile and soils.

Field Test

Nauroy et al. (1985a, 1985b) have performed a field grouted pile test in cemented calcareous soil. The test pile was a steel tube of 16 m long, 220 mm OD and 10 mm wall thickness grouted into a 310 mm diameter hole. Fig. 10 shows the details of the soil profile at the test site and the instrumented pile. The soil parameters E_s, τ_s and α have been backfigured from the static pile test, giving values of 200 MPa, 0.2 MPa and 1.0 respectively. The remaining soil parameters required in the analysis are assumed to be the same as those shown in Table 2.

The pile was subjected to five "parcels" of cyclic loading as shown in Fig. 11. The measured result indicates that the effect of the cyclic load (P_c) level is much more significant than the mean load (P_o) level in the accumulation of cyclic displacements. This behaviour is consistent with the assumption used in equation (4). The predicted and measured results are in fair agreement.

Table 2 Parameters used for Non-Linear Analysis.

Parameter	Value
E_m	60 MPa
τ_f	0.1 MPa
α	9.0
R	3.2
λ	0.25
$D_{r\,lim}$	0.06
θ	0.02

Note : The data used in the cyclic-displacement controlled degradation model is shown in Fig.5 for model pile tests.

BEHAVIOUR OF HYPOTHETICAL OFFSHORE PILE

The analysis has been employed to study the behaviour of a hypothetical offshore grouted pile subjected to the complete design storm loading as shown
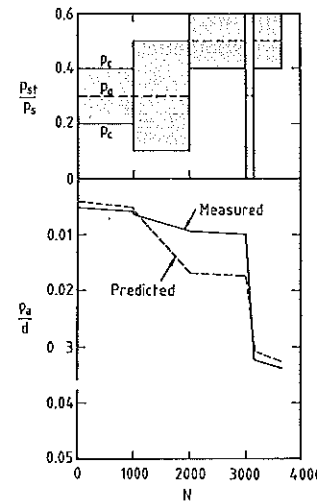
Fig. 11 Comparison of measured and prediction on field test (Nauroy et al. 1985 a, 1985 b).

in Table 3, using the same soil parameters listed in Table 2. This storm loading sequence is typical of a design storm for the North West Shelf of Australia. The offshore grouted pile is 60 m long and 2 m in diameter and is embedded in a uniform calcareous soil. The pile behaviour is examined for the original storm loading and two additional storm loadings developed by factoring up the original storm loading by factors of 1.5 and 2.0.

Fig. 12 shows that under the original storm loading, the rate of increase in pile displacement with number of cycles is small and almost constant. At the end of the original storm (i.e. after 8373 cycles) the pile has only settled about 0.02d. There is no degradatio° .of skin friction and the average degradation of soil secant modulus is only about 3% during the storm loading. The pile head stiffness (i.e. cyclic load divided by cyclic displacement of pile head) has reduced from 1452 kN/m to 1368 kN/m during the storm.

When the original design storm loading is increased by 50%, the general behaviour of the pile is unchanged and the pile displacement at the end of the storm loading only increases by about 20%, as shown in Fig. 13. There is again

Table 3 Details of the Original Storm Loading for Hypothetical Pile.

Parce l No.	No. of Cycles	Mean Load $\frac{}{P_s}$	Cyclic Load $\frac{}{P_s}$
1	2000	0.196	0.011
2	1600	0.199	0.014
3	1200	0.201	0.018
4	1000	0.204	0.021
5	780	0.207	0.025
6	560	0.211	0.030
7	410	0.214	0.034
8	290	0.218	0.038
9	200	0.222	0.043
10	120	0.226	0.048
11	90	0.230	0.053
12	51	0.234	0.059
13	32	0.239	0.065
14	20	0.244	0.070
15	10	0.248	0.076
16	6	0.253	0.082
17	3	0.258	0.088
18	1	0.267	0.100

P_s = ultimate static pile capacity

no degradation of skin friction and the average degradation of soil secant modulus is about 4% during the storm loading. The pile head stiffness has reduced from 1450 kN/m to 1345 kN/m. These results indicate that the induced pile loads are still mainly within the elastic region of pile response.

Fig. 14 plots the results of the design storm loading factored up by 2.0. The rate of increase in pile displacement increases with number of cycles, especially for more than 6000 cycles. The pile appears to have effectively failed due to accumulation of permanent displacement (i.e. $\rho_a \geqslant 0.1d$) at the end of the storm loading sequence. The average reduction in soil secant modulus at the end of the storm loading is 7% but again without any degradation in skin friction. The pile head stiffness decreases from 1449 kN/m to 1218 kN/m, but now the induced
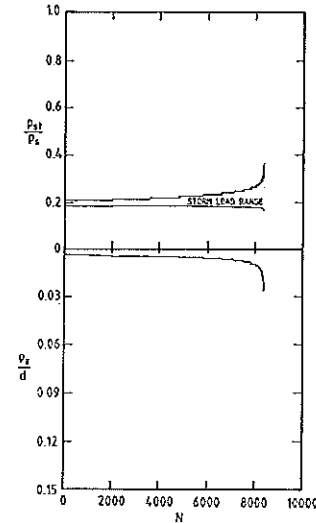
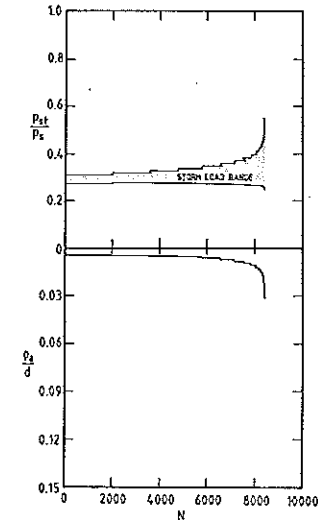**Fig. 12 Offshore pile subjected to design storm.**

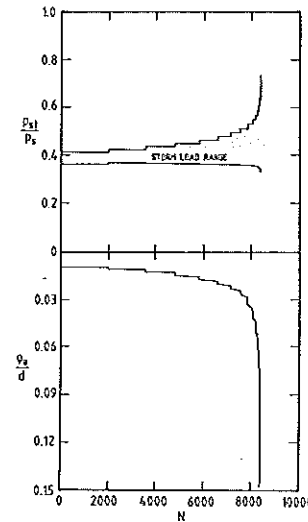**Fig. 13 Offshore pile subjected to design storm x 1.5.**

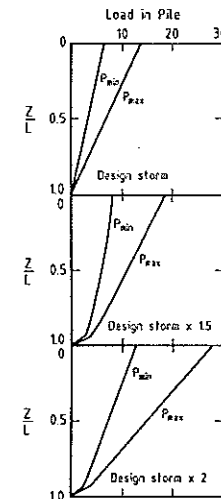**Fig. 14 Offshore pile subjected to design storm x 2.**

Fig. 15 Load distributions at the end of storm loadings.

pile loads are generally beyond the elastic range, resulting in increased pile settlement.

Fig. 15 plots the distributions of maximum and minimum loads predicted along the pile length for the three different design storm loadings. It can be seen that the slope of the load distribution curve becomes less steep with increasing storm loading, implying that greater shear stress along the pile is mobilised, with consequently larger pile settlements.

Fig. 16 shows the effect of an initial small "parcel" of cycling loading (S1) on the following larger "parcels" (S2), where S2 is, in turn, 1.5, 2 and 3 times the value of S1. When S1 is 10% of the pile capacity, the rate of accumulation of displacement during S2 remains almost unchanged until the latter is three times larger than S1. However, if S1 is increased to 20% of the pile capacity, the rate of accumulation of displacement during S2 increases significantly when S2 is twice S1, as shown in Fig. 17. This indicates that there is some influence on the cyclic behaviour of a pile from its previous cyclic loading history.
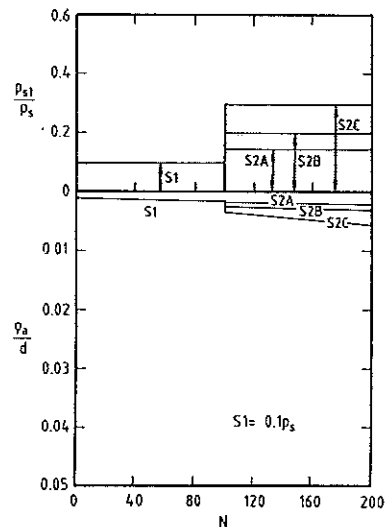

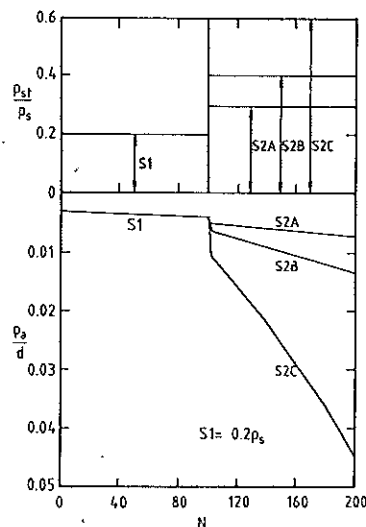**Fig. 16   Effect of smaller loading
history on pile behaviour.**

**Fig. 17   Effect of larger loading
history on pile behaviour.**

CONCLUSIONS

The results of the model pile tests indicate that the rate of accumulation of pile displacement increases as the magnitude of the storm loading increases. Failure during the storm was observed for a loading of twice the design value.

The non-linear analysis is able to predict the general trends of behaviour of the model pile tests under three different storm loadings with the soil parameters determined from earlier tests. The analysis is also able to simulate the general cyclic behaviour of a field grouted pile test in cemented calcareous soil. However, it does not always accurately predict the variations of pile displacement with number of cycles.

Using the same soil parameters as in the model tests, the theoretical behaviour of a hypothetical offshore pile under three different complete storm loadings has been studied and it is found that the behaviour is similar to that observed in the model tests. It is found that this pile is able to withstand the original design storm loading with a maximum displacement of only about 2.5% of the pile diameter.

ACKNOWLEDGEMENT

REFERENCES

DEANE, R., SHADE, D., SCHRIER, W. & WILLIAM, A. F. (1988). Development Implementation of Grouted Section Tests. *Int. Conf. on Calcareous Sediments*, Vol. 2, pp. 485-492.

HARA, A. (1980). *Dynamic Deformation Characteristic of Soils and Seismic Response Analyses of the Ground*. Dissertation submitted to the University of Tokyo.

HULL, T.S., POULOS, H.G. & ALEHOSSEIN, H. (1988). The Static Behaviour of Various Calcareous Sediments. *Proc. Int. Conf. on Calcareous Sediments*, Perth, Vol. 1, pp. 87-96.

LEE, C.Y. & POULOS, H.G. (1990a). Experimental Investigations of Axial Capacity of Model Grouted Piles in Marine Calcareous Sediments. *Research Report No. 618*, School of Civil and Mining Engineering, University of Sydney, Australia.

LEE, C.Y. & POULOS, H.G. (1990b). Tests on Model Instrumented Grouted Piles in Offshore Calcareous Soil. *Research Report No. 622*, School of Civil and Mining Engineering, University of Sydney, Australia.

LEE, C.Y. & POULOS, H.G. (1990c). Analysis of Axially Loaded offshore Grouted Piles. Submitted to Jnl. Numerical and Analytical Methods in Geomechanics.

MASING, G. (1926). Eigenspannungen and Verfestigung beim Messing. *Proc. 2nd Int. Congress of Applied Mechanics*, pp. 332-335.

MATLOCK, H. & FOO, S.C. (1979). Axial Analysis of Piles Using a Hysteretic and Degradation Soil Model. *Proc. Conf. Num. Meths. in Offshore Piling*, Inst. Civ. Engrs, London, pp. 165-185.

NAUROY, J.F. & LE TIRANT, P. (1985a). Driven Piles and Drilled and Grouted Piles in Calcareous Sands. *Proc. 17th Annual Offshore Technology Conference*, OTC Paper 4850.

NAUROY, J.F., BRUCY, F. & LE TIRANT, P.C. (1985b). Static and Cyclic Load Tests on a Drilled and Grouted Pile in Calcareous Sand. *Proc. 4th Int. Conf. on Behaviour of Offshore Structures*, (Boss '85).

POULOS, H.G. (1989). Cyclic Axial Loading Analysis of Piles in Sand. *Journal of the Geotechnical Engineering Division, ASCE*, Vol. 115, No. 6. pp. 836-852.

POULOS, H.G. & LEE, C.Y. (1988). Model Tests on Grouted Piles in Calcareous Sediment. *Int. Conf. on Calcareous Sediment*, Perth, Vol. 1, pp. 255-260.

POULOS, H.G. & LEE, C.Y. (1989). Behaviour of Model Grouted Piles in Offshore Calcareous Sand. *Proc. 12th Int. Conf. on Soil Mechanics and Foundation Eng*, pp. 955-958.

PYKE, R. (1978). Nonlinear Soil Models for Irregular Cyclic Loadings. *Journal of Geotechnical Engineering Division, ASCE*, Vol. 105, G76, pp. 715-726.

RAMBERG, W. & OSGOOD, W.T. (1943). Description of Stress-Strain Curves by Three Parameters. *Tech. Note 902*, National Advisory Committee for Aeronautics.